

4. M. Chi and S. Basu. Analytical Study for Fatigue of Highway Bridge Cables. Report FHWA/RD-81/090. FHWA, U.S. Department of Transportation, July 1981.
5. K. Harada et al. Aeolian Vibration of Conductor and Its Suppression Method. The Hokkaido Electric Power Company, Inc., April 1968.
6. R.A. Komenda. Wind Excitation of Stranded Cable. Preformed Line Products Company, Cleveland, Ohio, 1974.
7. H.C.S. Thom et al. Wind Forces on Structures. Paper 3269. Transactions, ASCE, Vol. 126, Part II, 1961.
8. J.M. Kulicki. Aerodynamically Induced Vibrations of H-Shapes for the Second Newburgh-Beacon Bridge (Deck Truss Spans). Modjeski and Masters, Harrisburg, Pa., April 1976.
9. R.H. Scanlan and R.L. Swart. Bending Stiffness and Strain in Stranded Cables. Conference Paper 68 CP 43-PWR. IEEE Winter Power Meeting, New York, 1968.
10. H.S. Reemsnyder. The Mechanical Behavior and Fatigue Resistance of Steel Wire, Strand, and Rope. Report of the Ad Hoc Committee on Mechanical Rope and Cable, National Materials Advisory Board, National Research Council, Washington, D.C., 1972.
11. J.W. Fisher and I.M. Viest. Fatigue Tests of Bridge Materials of The AASHTO Road Test. Special Report 66, HRB, National Research Council, Washington, D.C., 1961.
12. J.W. Fisher. Bridge Fatigue Guide Design and Details. American Institute of Steel Construction, New York, 1977.

Publication of this paper sponsored by Committee on Steel Bridges.

Finite Element Analysis of Cracked Diaphragm Welds on the Ohio River Bridge at Wheeling, West Virginia

JOHN M. KULICKI, STEVEN W. MARQUISS, and RALPH J. DeSTEFANO

ABSTRACT

This paper contains a discussion on the finite element analysis of cracks in welds connecting floorbeam back-up diaphragms and web plates of box tie girders in a tied-arch bridge. Comparisons of the finite element analysis and the field instrumentation results are made at selected locations, and for one typical position of a test truck. Drawing on the conclusions of the finite element analysis, contract plans were developed to retrofit the tie girder. Two previously unconnected edges of the diaphragms were connected to the top and bottom flanges of the tie girder. Also, the floorbeam bottom flange was connected directly to the tie girder bottom flange.

Two terms are used in this paper that require definition:

- Web gap: The space left between partial-depth, tie girder diaphragms and a tie girder flange.
- Floorbeam gap: An area of incomplete or non-existent contact between a floorbeam end plate and a tie girder web.

In March 1983, a West Virginia Department of Highways inspector made a routine inspection of the unopened, tied-arch Bridge Number 2494, which enables Interstate 470 to cross the Ohio River at Wheeling, West Virginia. A recurring pattern of weld cracking

was observed during the inspection of the interior of one of the 780-ft Langer Girder arch ties. The detail involved was a fillet-welded connection of the floorbeam diaphragm and the exterior tie girder web. The interior web connection to the diaphragm was an end plate detail bolted through the tie girder web and a floorbeam end plate. Sealing diaphragms, approximately 5 ft 2 in. on each side of each floorbeam diaphragm, extended to the top and bottom tie girder flanges (no web gaps) and similar cracking was not found in these diaphragms. A Plan and Elevation view of the bridge, taken from the original designer's drawings, is shown in Figure 1 and the typical cracked diaphragm weld is shown in Figure 2.

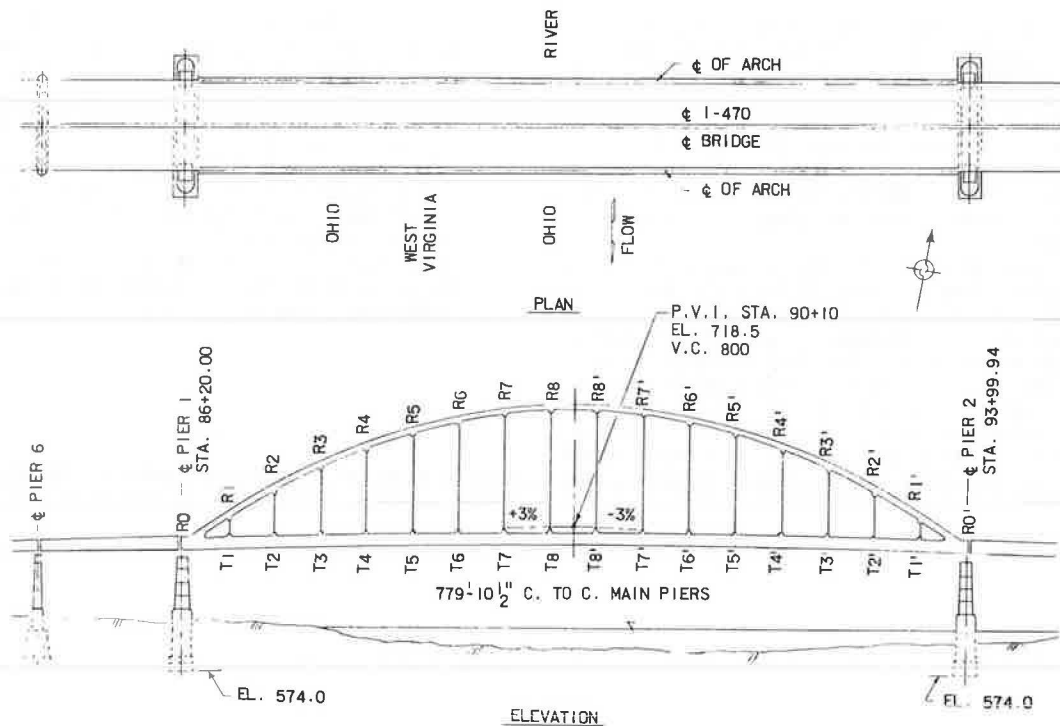


FIGURE 1 Plan and elevation of Bridge Number 2494.

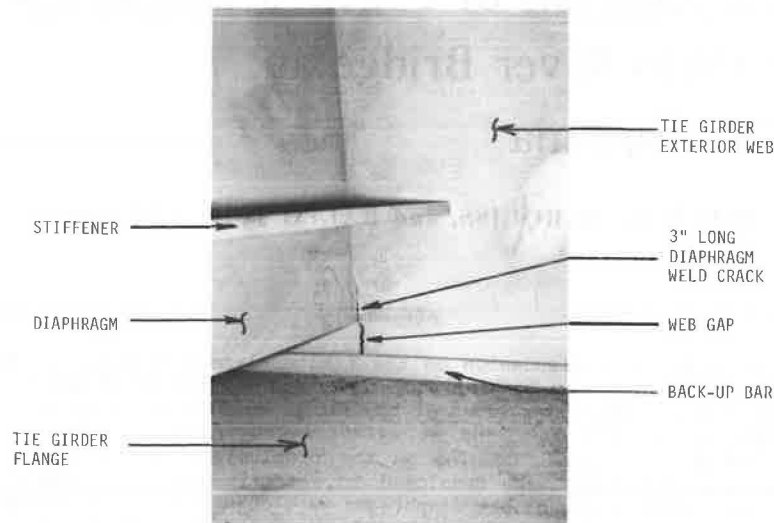


FIGURE 2 Diaphragm fillet weld cracks discovered in March 1983.

The West Virginia Department of Highways authorized Modjeski and Masters to undertake experimental and analytical stress studies to identify the cause of the weld cracking. Modjeski and Masters engaged Dr. John W. Fisher of Lehigh University to direct the experimental work, which began in September 1983 and involved strain gauge monitoring of the areas adjacent to the diaphragm fillet welds. Referring to Figure 2, this included the unsupported, exterior tie girder web immediately below the diaphragm and a similar unsupported web region at the top of the 12-ft-tall box girder. In addition, strain gauges were mounted on the interior tie girder web below the floorbeam-diaphragm connection. The diaphragm and flanges were also monitored; the top interior web, however, was not. The results of the experi-

mental work will be reported only as they relate to the finite element analysis.

In an unpublished interim report dated September 1983, Dr. Fisher indicated that extrapolation of the web gap stresses (reduced from the strain measurements) to the web-flange weld root implied high stress ranges at the weld root. This raised the possibility of fatigue crack development in the web, as illustrated by Figure 3, a problem potentially more serious than the diaphragm fillet weld cracking. Several small cracks were found when seven lengths of back-up bar were removed so that the weld root could be examined.

The primary objective of the study reported herein was to perform a comprehensive finite element analysis of the tie girder-floorbeam connection

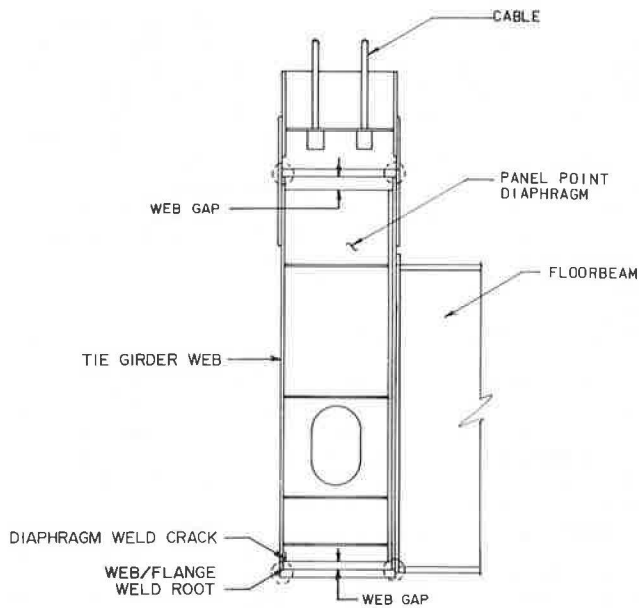


FIGURE 3 Web/flange weld root fatigue cracking.

detail. Particular emphasis was devoted to the web gap regions, so that a retrofit could be designed that would arrest the development of additional diaphragm weld cracks and prevent the development of fatigue cracks at the web-flange weld root.

The proposed retrofit that evolved from the finite element analysis took two forms (see Figure 4). The first was a mechanical connection between the floorbeam diaphragm and the tie girder flanges to provide a four-sided connection rather than the present two-sided connection. Several variations of this type of retrofit were studied. All variations will be referred to as "diaphragm retrofits" in the following text. The second form of retrofit was an

additional mechanical connection between the bottom of the floorbeam and the tie girder flange. This will be referred to as the "bottom flange retrofit."

LOCATIONS STUDIED

Because the interaction of forces at the tie girder-floorbeam connection was complex, verification of the accuracy of the analytical finite element results through comparison with the field-measured response reported by Dr. Fisher was essential. Only Panel Points 4' and 8' of the north tie girder were strain-monitored; therefore, computer analysis of these locations was the logical choice. It was assumed that all results (analytic and experimental) were indicative of behavior throughout the bridge.

The loadings that produced the field-measured stresses consisted of two 80-k, 5-axle trucks traveling in adjacent westbound traffic lanes. For the analytical investigation, the wheel loads from these 80-k trucks were placed on a computer model of the bridge so as to produce the maximum response at Panel Points 4' and 8'. Following this, the wheel loads were individually distributed transversely through the slab to the individual stringers by assuming the deck to be simply supported at each stringer.

COMPUTER MODELS

Introduction

Because the object of this investigation was to study diaphragm connection details having dimensions of 1 to 5 in., the use of a modeling technique called "substructuring" was required. This technique utilized a conventional, space-frame analysis followed by several generations of finite element models. Each generation analyzed a successively smaller portion of the connection detail using successively closer nodal spacing. The preliminary models constructed with coarse nodal discretizations furnished

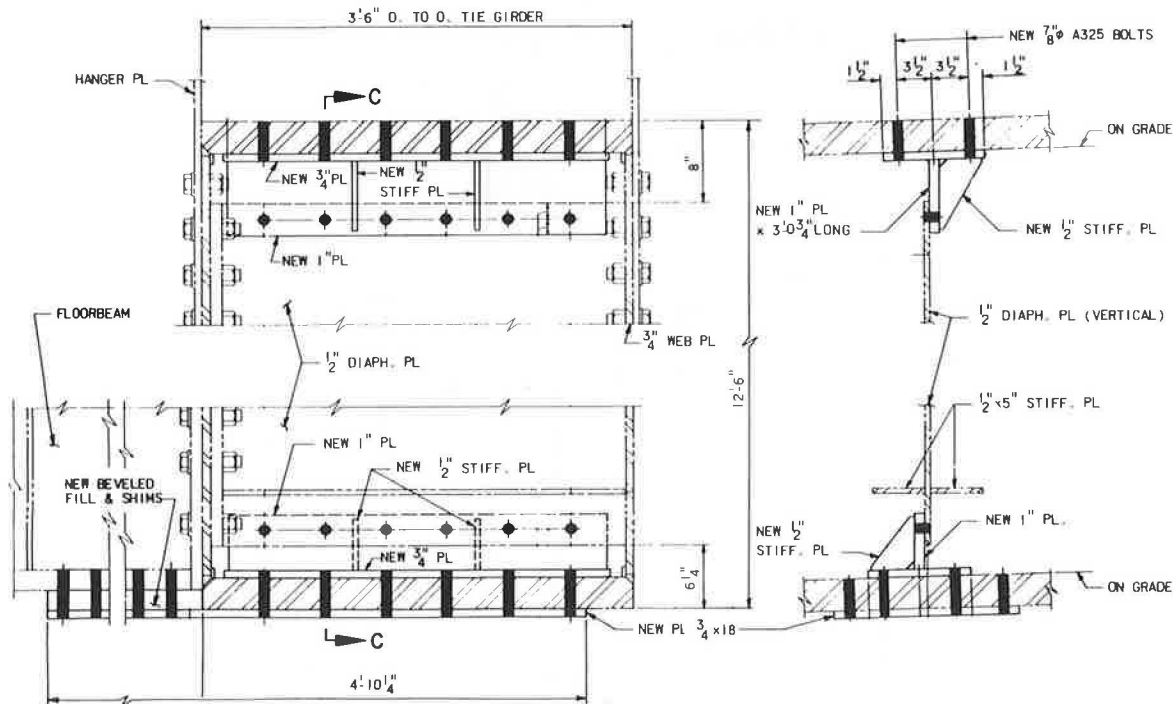


FIGURE 4 Diaphragm and floorbeam retrofits.

the forces and displacements for each subsequent model. In this manner, it was possible to use sufficiently small elements to achieve the desired analysis "sensitivity" in the final generation and still solve problems of manageable size. A flow chart of the substructuring used in this study is shown in Figure 5.

The first computer model utilized the "STRESS" computer program. The second, third, and fourth generation computer models were composed of three-dimensional, thin- and thick-shell finite elements. These models were analyzed using the "Static Analysis Program (SAP) for Three-Dimensional Solid Structures" developed at the University of California at Berkeley.

Finite Element Models

The first finite element model (see Figure 6) consisted of a portion of the tied-arch, box girder and a typical girder-floorbeam connection. The primary purpose of this model was to make a transition from the space-frame analysis to the finite element analysis (i.e., from a strength-of-materials approach to a theory-of-elasticity analysis). The model consisted of a sealing diaphragm located 5 ft 2 in. on either

side of a central floorbeam diaphragm, an interior and an exterior tie girder web, and the top and bottom tie girder flanges. A 5-ft section of the adjoining floorbeam was also attached to the floorbeam diaphragm. This model eventually represented two conditions: one with the web gap between the diaphragm and flanges (original condition) and one with the gap closed (retrofit condition).

Like most modern finite element programs, SAP permitted the use of different types of finite elements in the same model. The tie girder webs and all flanges were modeled as thin-shell elements. The diaphragms and floorbeam web were modeled with plane stress membrane elements, since they received no out-of-plane loadings.

This model was loaded with forces obtained from the space-frame model. As shown in Figure 7, nodal loads were applied to the floorbeam to account for the moment and shear present in the floorbeam section (axial load could be neglected) and at points on both the inside and outside tie girder webs to represent the forces in the suspender strands.

The equivalent nodal loads for the moment and shear in the floorbeam were found by assuming a linear stress distribution (i.e., $\sigma = MC/I$ and $T = V/bt$). Floorbeam nodal loads were computed by multiplying the stress by the territorial area of each node. The nodal loads representing the suspenders

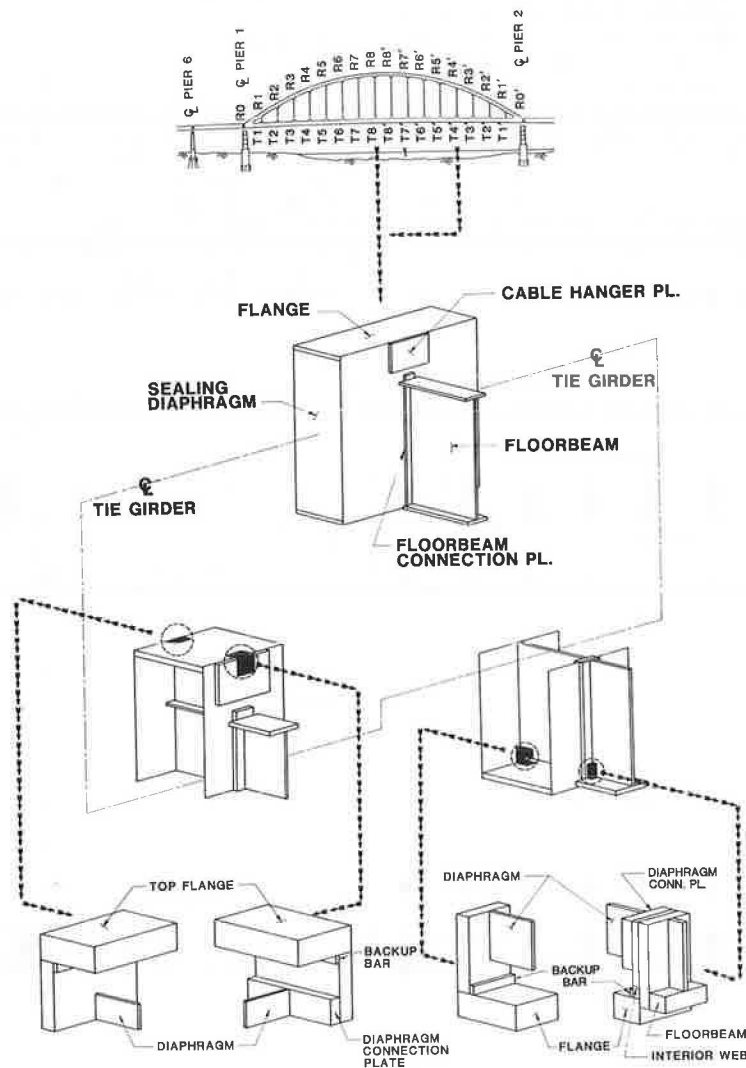


FIGURE 5 Computer model substructuring.

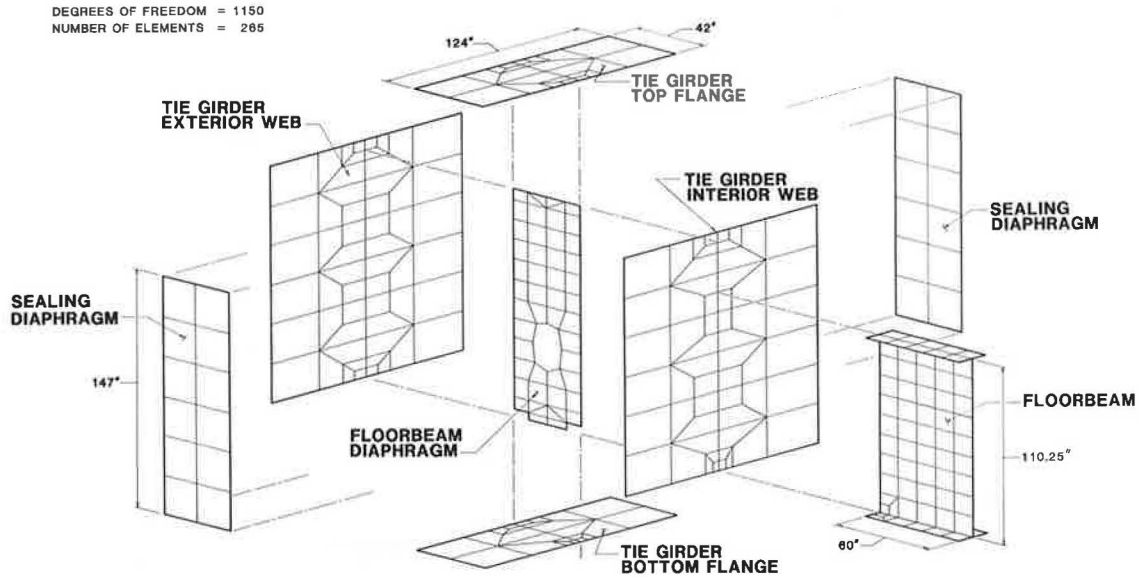


FIGURE 6 First finite element model.

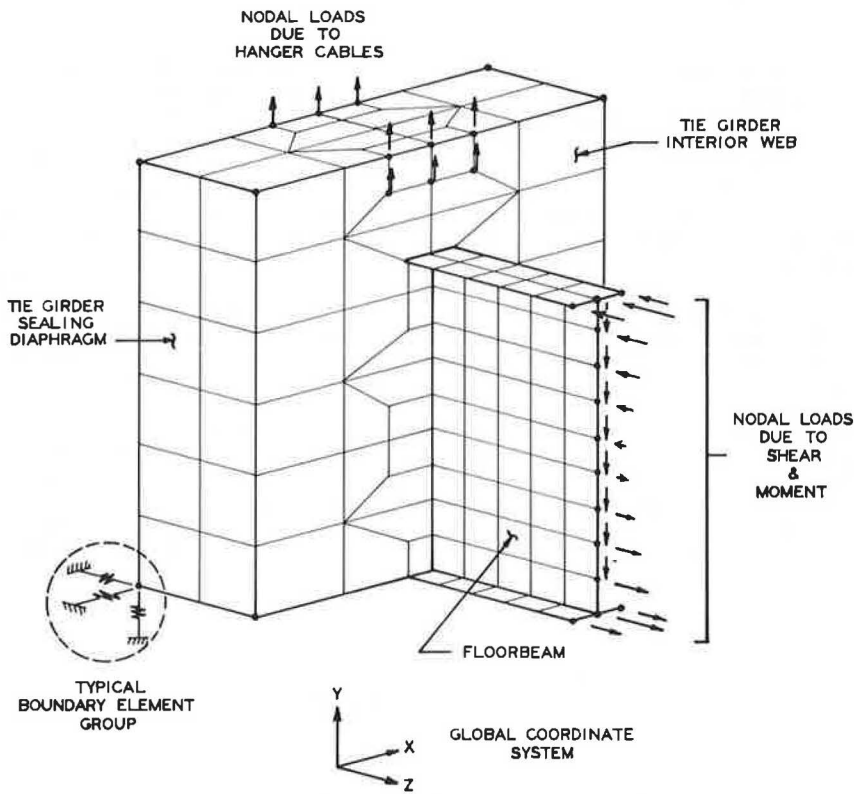


FIGURE 7 Constraints and loads applied to first finite element model.

were also obtained by uniformly distributing the axial forces in the suspenders among six nodes.

Stability of the model was provided by boundary elements. Boundary elements are unidirectional constraints that can create specified nodal displacements in any desired direction. Three boundary elements oriented to the global x, y, and z axes were placed at the four corner nodes of the two sealing diaphragms. Not only did these boundary elements stabilize the model, they also introduced torsion, moment, and axial forces into the tie girder by

displacing the structure. These boundary forces were consistent with the space-frame analysis.

Two second-level finite element models advanced the substructuring process by dividing the tie girder along its neutral axis for the separate investigation of the top and bottom web gaps. The finite element model of the bottom half of the tie girder is shown in Figure 8 (the model for the top half was similar). Like the first finite element model, this model eventually represented both the original and the retrofitted conditions.

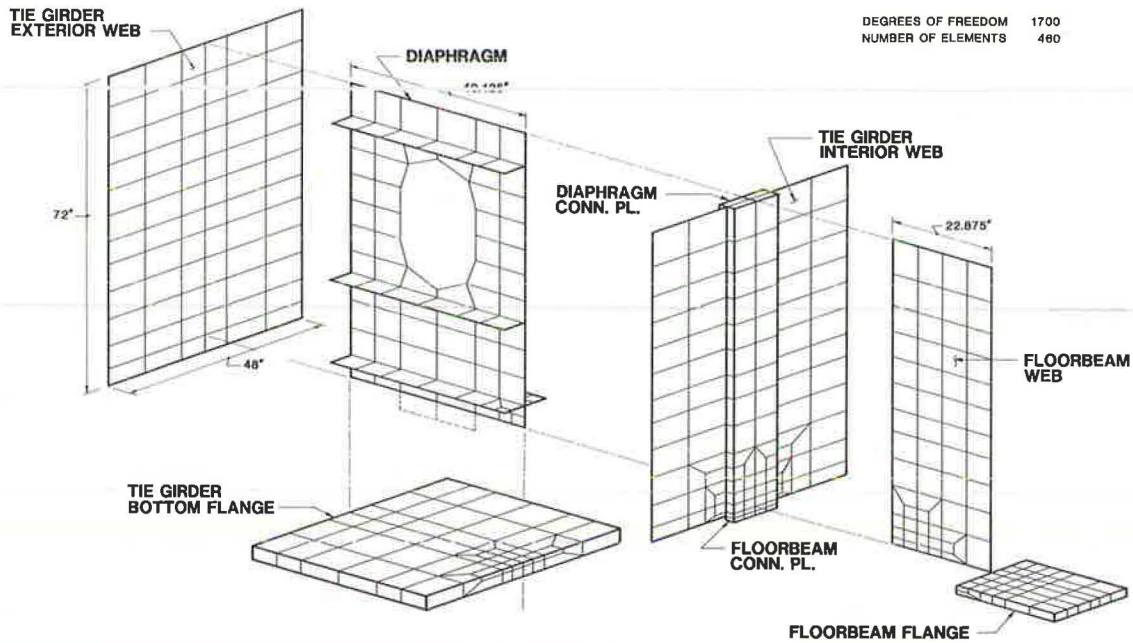


FIGURE 8 Second-level finite element model.

These second-level models confined the analysis to a region bounded by a line 2 ft on either side of the floorbeam diaphragm and by the tie-girder neutral axis. A 2-ft length of the floorbeam was again attached to the floorbeam diaphragm. Boundary elements were located at the corners of the box girder, along the neutral axis, and on the attached floorbeam.

With the increased elemental thickness-to-length ratios caused by the finer nodal discretization, the use of "brick elements" was preferable for all the flanges and the tie girder-floorbeam connection plates. (A brick element is a solid, three-dimensional element that effectively models the assemblage of plates utilized within the connection details.) The other model components remained as previously described.

The final substructuring of the tie girder-floorbeam connection was a set of four, third-level finite element models, one of which is shown in Figure 9. This model shows the finite element mesh for the bottom interior corner of the tie girder (the models

for the remaining tie girder corners were similar). Each of the four, third-level models focused on one of the tie girder's corner web gap regions, so that stress gradients along the interior surface of each web gap could be determined. By comparing the stress gradients obtained from these models with varying structural parameters (e.g., with and without retrofits), the effectiveness of various retrofit details could be evaluated.

The third-level models consisted almost entirely of solid, three-dimensional elements so that the most accurate representation of the web gap regions could be obtained. Stresses were induced in the models by imposing boundary element displacements obtained from the previous substructure models; there were no surface loads applied to the models. These boundary elements were located at the tie-girder flange below the web gap and along the floorbeam diaphragm above the web gap.

The only variations in modeling that were studied at this level of substructuring, without starting at

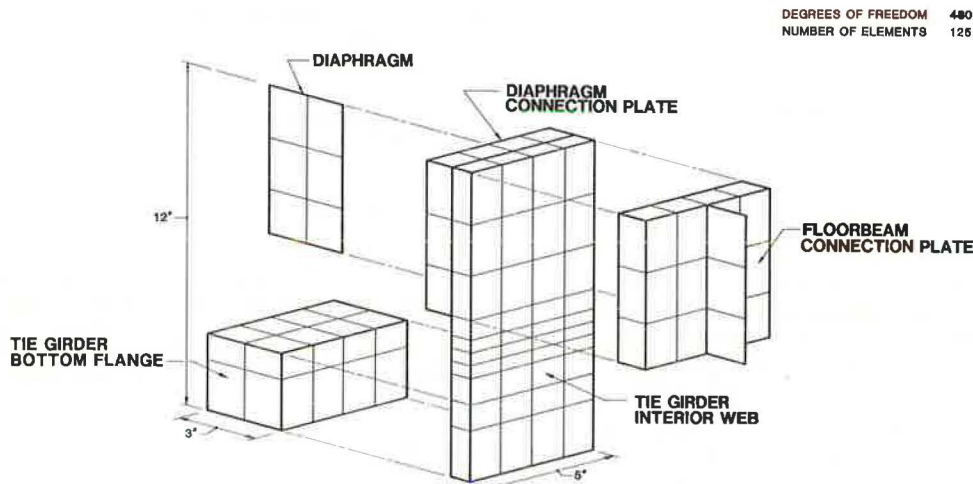


FIGURE 9 Third-level finite element model.

an earlier level, were the inclusion of the back-up bars and fillet welds between the tie-girder flange and web. All other parameters investigated (i.e., variations of the diaphragm retrofit and the bottom flange retrofit) were carried through all stages of substructuring to obtain the most accurate results possible with the procedure described previously.

ANALYTIC RESULTS

The results of the computer analysis will be presented in this section. First, the top and bottom web gap regions (i.e., four corners), at Panel Point 8 will be discussed without the retrofit installed, and then with the retrofit installed. This will be followed by a similar discussion of the bottom web gaps at Panel Point 4'. The top web gap region was not reanalyzed at Panel Point 4' because the experimentally measured stress gradients there were not significantly different from those obtained at Panel Point 8.

Obviously, fatigue of welded details is caused by a fluctuating stress (i.e., stress range). In evaluating both the accuracy of finite element models and the effectiveness of retrofits, no effort was made to reproduce both the positive and negative phases of the experimentally observed stress ranges. Rather, it was assumed that good agreement between measured and analytic results, and the analytically determined effectiveness of a retrofit obtained for one live load position, would also apply to other live load positions (i.e., superposition).

Panel Point 8 Results Without Retrofit

The deformations of the tie girder top and bottom web gap regions at Panel Point 8 without the diaphragm retrofit are shown in Figures 10 and 11. A differential displacement between the floorbeam

diaphragm and the tie girder flange equal to 0.00517 in. occurred within the top web gap region. The bottom web gap displacements were much smaller. Nevertheless, in gap details, displacements of even this small order of magnitude characteristically cause high stresses. Conclusions as to the mechanism causing the web gap stresses were drawn by analyzing these deformations.

In both the top exterior and top interior web gaps, it was evident that the out-of-plane translation of the diaphragm relative to the tie girder flange induced most of the web gap stresses. Although some rotation occurred in both the flange and diaphragm, the rotation had the effect of reducing the stresses in the web, rather than increasing them. Comparison of the stress gradients obtained from the finite element analysis with those measured experimentally are shown in Figures 12 and 13.

In Figure 12, experimentally measured stresses in the top exterior web gap varied from -2 ksi (compression) at the back-up bar to +4 ksi (tension) at the top of the diaphragm. The analytical stresses (without retrofit) varied between -4 ksi and +4 ksi. The top interior web gap was not strain-gauged; however, analytical stresses obtained at this location (see Figure 13) varied between +3 ksi at the back-up bar and -2 ksi at the top of the diaphragm. This reversal in sign of the web stresses through the gap length was expected in light of the displacements shown by Figure 10.

Similarly, the bottom exterior web gap experimentally measured stresses at Panel Point 8 varied between -2 ksi at the bottom of the diaphragm and +3 ksi at the web-flange weld root as shown in Figure 14. This response was also observed in the finite element model that yielded a stress variation from -.5 ksi to +4 ksi in the same region.

The bottom interior web gap--the fourth and final location studied at Panel Point 8--showed a structural response different from the previous three web

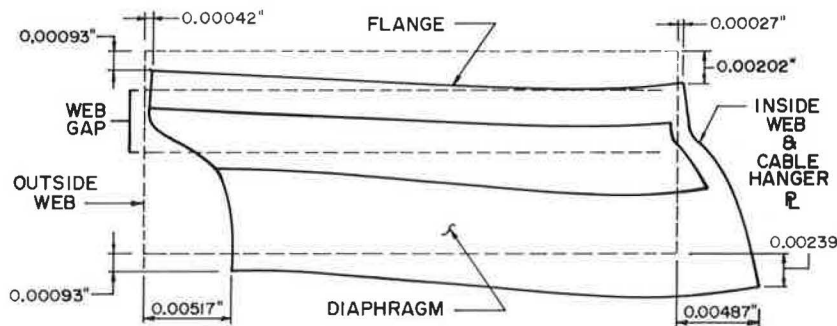


FIGURE 10 Top web gap deformation without retrofit at Panel Point 8.

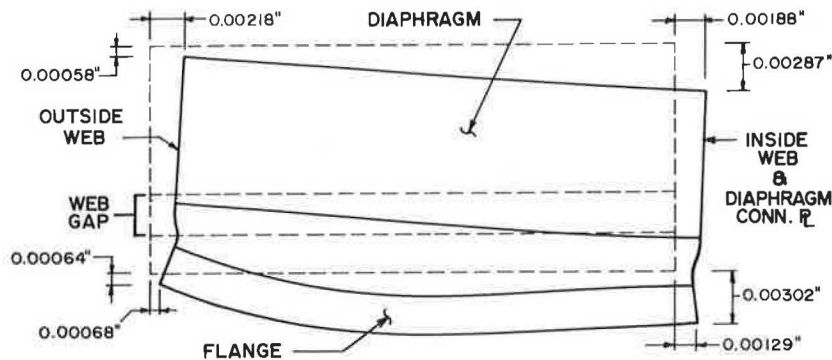


FIGURE 11 Bottom web gap deformation without retrofit at Panel Point 8.

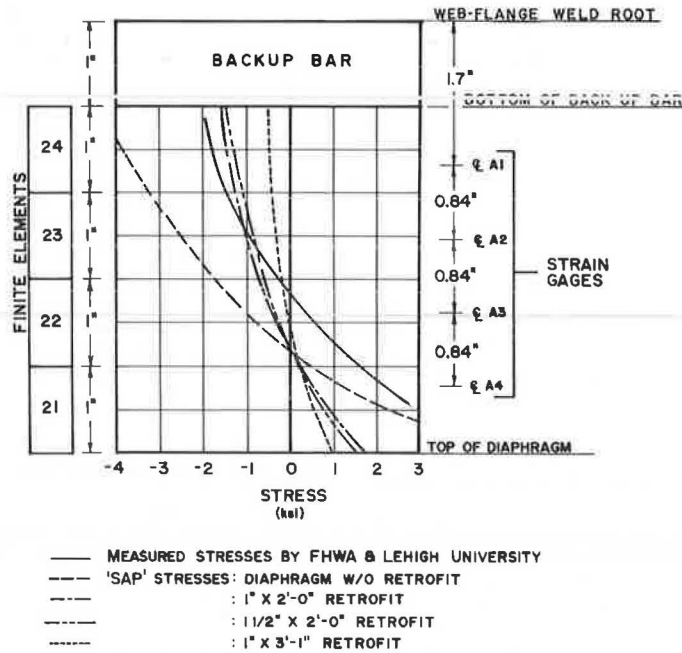


FIGURE 12 Stress gradients in top exterior web gap at Panel Point 8.

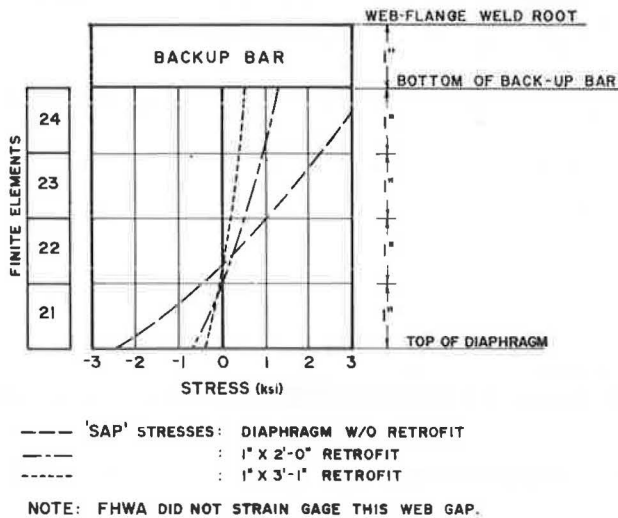


FIGURE 13 Stress gradients in top interior web gap at Panel Point 8.

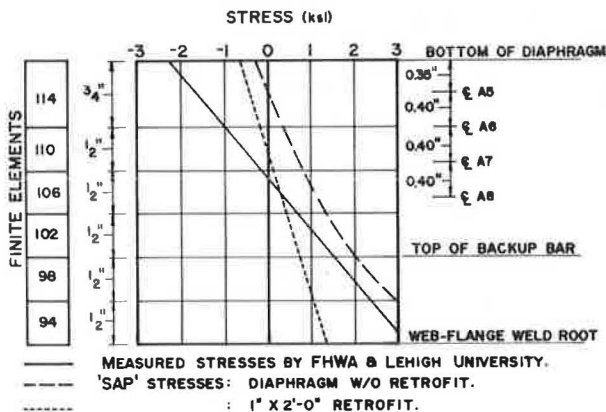


FIGURE 14 Stress gradients in bottom exterior web gap at Panel Point 8.

gaps described. Here, the measured stresses (see Figure 15) indicated that there was no change in the direction of applied moment along the entire web gap surface. All previous web gaps showed change in sign of static stresses within the gap. The initial analytical results at this web gap indicated that this type of behavior (change in sign of stresses) could be expected here also. Clearly, some improvement in the modeling of the bottom interior web gap was needed.

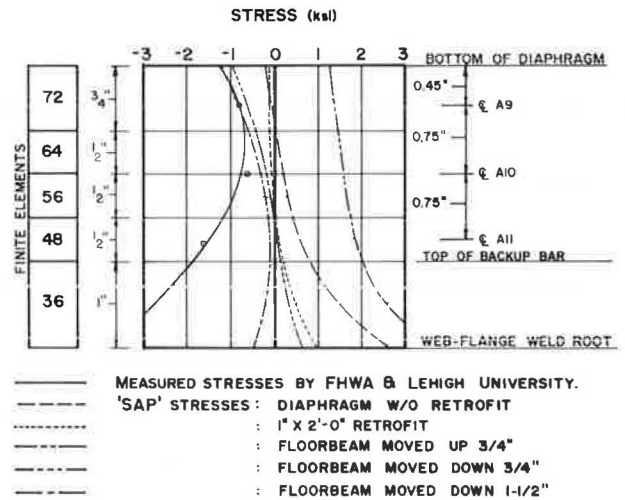


FIGURE 15 Stress gradient in bottom interior web gap at Panel Point 8.

In an attempt to reproduce the measured values on the entire web gap surface, the floorbeam was analytically repositioned vertically so as to introduce an eccentric loading into the flange and cause the rotation of the flange necessary to produce the experimentally measured stress variation. However, when the stresses did not match the measured values even with the floorbeam flange lowered 1.5 in., it

became obvious that some other phenomenon was precipitating the experimental results, because no misalignment of the indicated magnitude was observed in the field. It is important to note here that all connection details discussed previously were modeled as designed (i.e., the floorbeam flange was assumed to bear perfectly against the tie girder flange).

It was evident that still another modification to the original model was needed to resolve the bottom interior stresses. It was therefore decided that concentration should be on the bottom interior web stresses at Panel Point 4', since those experimentally measured stresses were much higher than those at Panel Point 8. The results obtained at Panel Point 4' will be discussed later, and an explanation for the difference in behavior between the bottom exterior and interior corner will be presented.

Panel Point 8 Results with Diaphragm Retrofit

Figures 16 and 17 show, respectively, the deformations of the top and bottom web gap regions with the most effective diaphragm retrofit installed. This retrofit is a T-section fabricated from 1-in. plates bolted to the tie girder diaphragm and flange, thus effectively filling the gap between these structural elements.

Figures 12 and 13 show the reduction in stresses for the top exterior and interior web gaps caused by varying the length and thickness of the retrofit. As expected, the retrofit that provided the maximum shear stiffness between the translating diaphragm and the rigid tie girder flange reduced the stresses most significantly (i.e., the 3 ft 1 in. retrofit). The analytical stresses at the top exterior web gap were reduced to -0.5 ksi at the back-up bar and $+1$ ksi at the top of the diaphragm. A similar reduction

of stresses was observed at the top interior web gap with the 3 ft 1 in. retrofit. The 2-ft retrofit was found to be adequate for the bottom exterior and interior web gaps at Panel Point 8 and was not re-analyzed with the 3 ft 1 in. retrofit as an expedience. In the top web gaps, it became evident that the ability of diaphragm retrofit to almost completely eliminate the rotation and translation between the tie girder flange and the floorbeam diaphragm was the primary reason why it was effective in reducing the web gap stresses.

Panel Point 4' Results Without Retrofit

As stated previously, the previous results at Panel Point 8 led to the hypothesis that (a) the connection detail was not acting as designed, and (b) vertical misalignment of the floorbeams was an improbable cause, since analytical stresses of the indicated magnitude did not result from this misalignment.

It was clear, then, that some other mechanism had to be responsible for such high stresses. It was deduced that the only way to simultaneously obtain the measured stress gradients in both the exterior and interior web gaps was for the force from the floorbeam to be transmitted directly into the diaphragm. This would cause a net reduction of length of the bottom of the diaphragm combined with a local rotation at the interior bottom corner of the diaphragm, as shown in Figure 18. As a result of this reasoning, it became apparent that the floorbeam must not be bearing against the tie girder flange at the two panel points that were instrumented (and probably elsewhere). This lack of bearing between the floorbeam and the tie girder was called "the floorbeam gap" as shown in Figure 19.

The floorbeam gap was first assumed to extend to

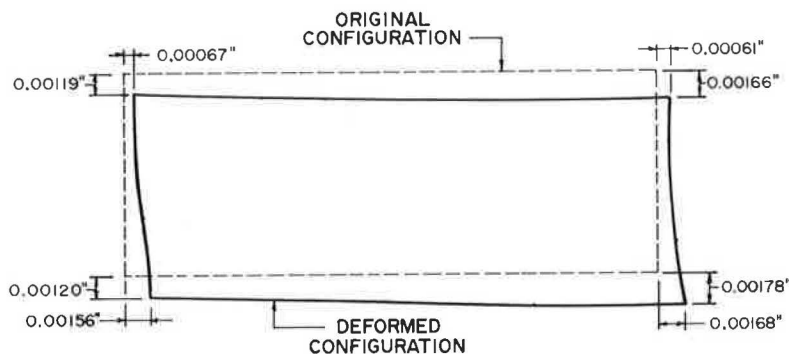


FIGURE 16 Top web gap deformation with retrofit at Panel Point 8.

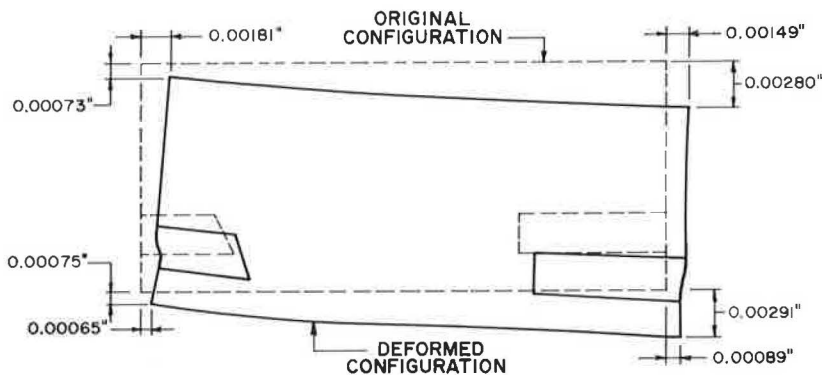


FIGURE 17 Bottom web gap deformation with retrofit at Panel Point 8.

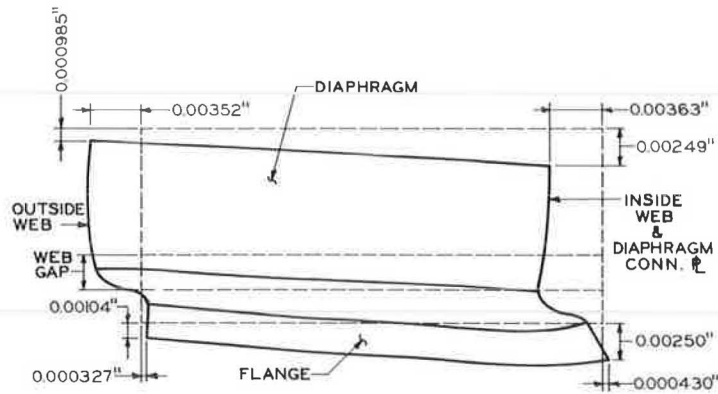


FIGURE 18 Bottom web gap deformation without retrofit at Panel Point 4'.

the bottom of the diaphragm. This gap length produced a stress gradient (see Figure 20) on the inside web surface ranging from -14 ksi at the web-flange weld root to +12 ksi at the bottom of the diaphragm. Reducing the floorbeam gap length to the web gap midpoint (by increasing the connection plate length) concentrated the web translation and rotation at the web-flange weld root and increased the stresses accordingly, as shown in Figure 21. This second set of stresses contained weld root tensile stresses

significantly greater than those previously modeled or measured.

In summary, the best match between measured and calculated stresses resulted when the inferred floorbeam gap was assumed to extend from the bottom flange of the floorbeam to the bottom edge of the tie girder diaphragm. This gap could not be physically confirmed, and is more academic than consequential after the retrofit is installed. Figure 22 shows the bottom exterior web gap stresses at

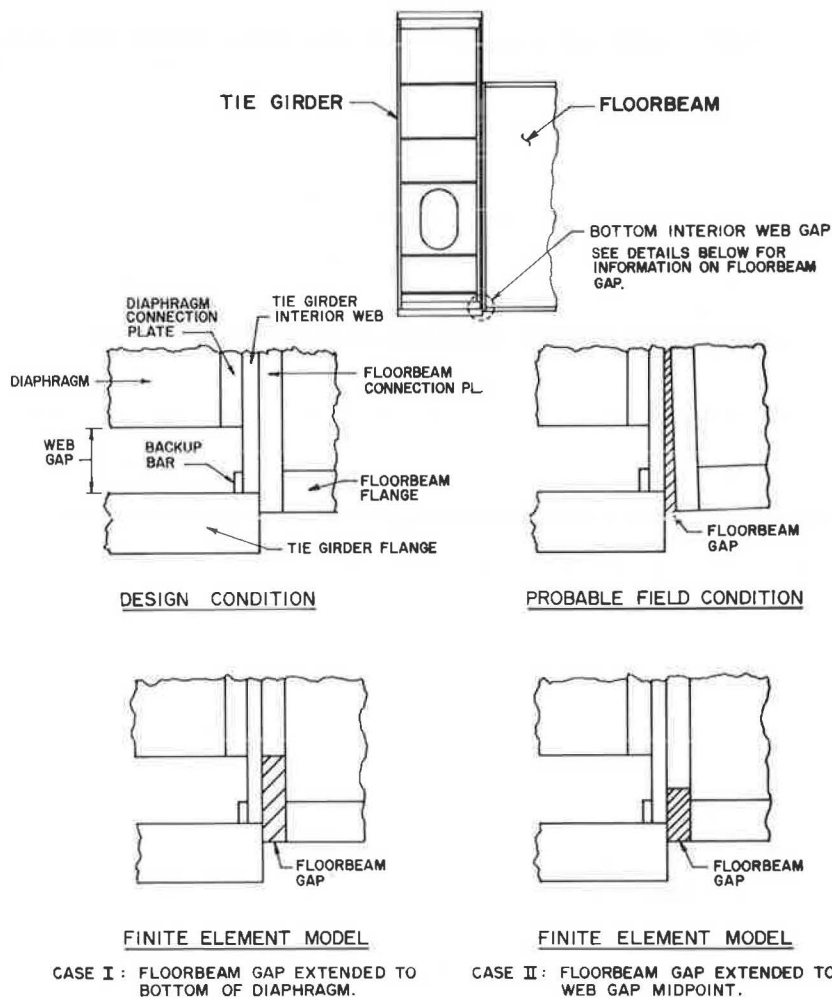


FIGURE 19 Floorbeam gap configurations.

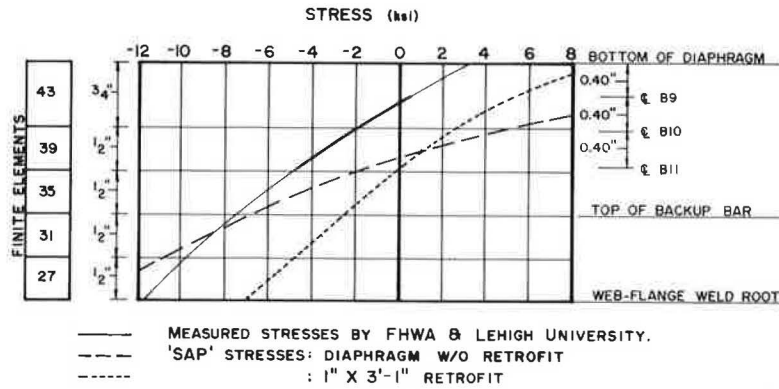


FIGURE 20 Stress gradients in bottom interior web gap at Panel Point 4'—floorbeam gap extended to bottom of diaphragm.

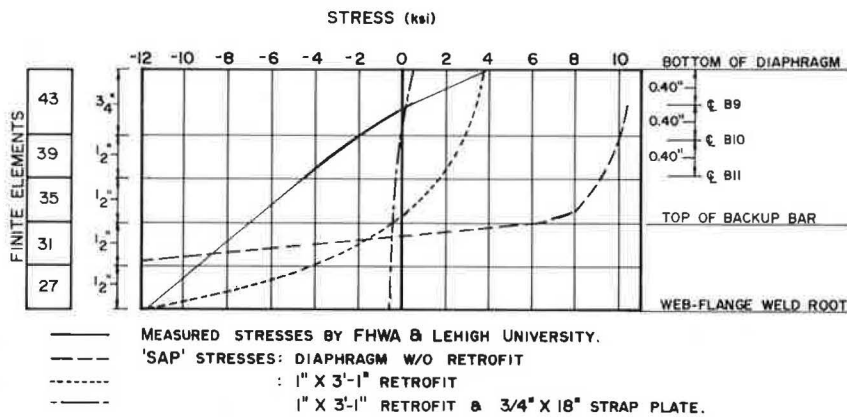


FIGURE 21 Stress gradients in bottom interior web gap at Panel Point 4'—floorbeam gap extended to web gap midpoint.

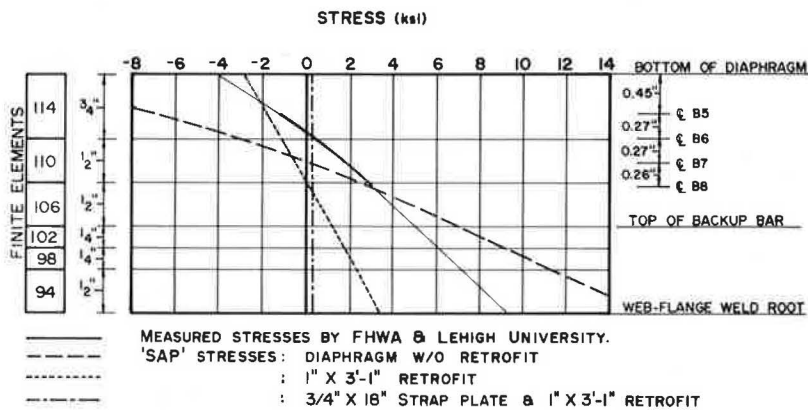


FIGURE 22 Stress gradients in bottom exterior web gap at Panel Point 4'.

Panel Point 4' with the floorbeam gap assumed to extend to the bottom of the diaphragm. Good agreement with the measured stresses is evident. Variations in the floorbeam gap length did not affect the bottom exterior web gap displacements and, inferentially, would not be expected to affect the resulting stresses.

Panel Point 4' Results with Diaphragm Retrofit

Figures 20 and 21 show the interior web stress gradients for the two floorbeam gap lengths with a dia-

phragm retrofit installed. For the case in which the floorbeam gap extended up to the bottom of the diaphragm (Figure 20), a stress reduction to one-half of the original values at the bottom interior web-flange weld root was observed. The most critical case (the floorbeam gap extended to the web gap midpoint, which is shown in Figure 21) has a stress range between 15 and 20 ksi. Thus, the 3 ft 1 in. retrofit did not adequately reduce the stress range at the bottom interior web gap at Panel Point 4'. The floorbeam gap apparently caused transfer of all the load through the floorbeam diaphragm. A positive means of forcing the load directly into the tie

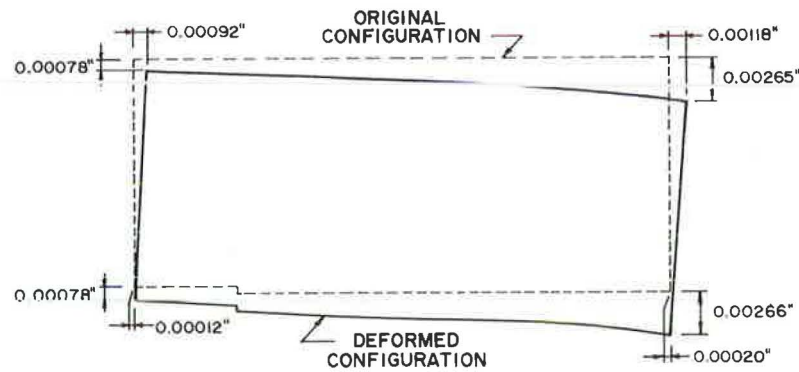


FIGURE 23 Bottom web gap deformation with retrofit and tie plate at Panel Point 4.

flange without passing through the diaphragm was required.

The bottom exterior web gap stresses (see Figure 22) were reduced to approximately one-fifth of their original value by the displacement-reducing action of the diaphragm retrofit. Even though this was a significant decrease, the stress range was still relatively high (i.e., approximately 7 ksi).

Results with Diaphragm Retrofit and Tie Strap Plate

It was found that the installation of a structural plate (tie strap) bolted to the tie girder and floorbeam bottom flanges would adequately reduce the stresses and web deformations, as shown in Figures 21-23. It is important to note that the combined floorbeam and diaphragm retrofits reduced the stress range to approximately 1 ksi on the bottom interior web gap (see Figure 21), which previously had exhibited a stress range of 15 to 20 ksi; thus, the bottom exterior web gap bending stresses (see Figure 22) were essentially eliminated. The combined effect on top gap stresses was not significantly different from the effect of the diaphragm retrofit alone.

Back-Up Bar and Fillet Weld Effects

The presence of a back-up bar in the corners of the tie girder raised some questions about the accuracy of the modeling. Several analyses were made to study the effect to assure that the worst condition was investigated and corrected by the retrofit procedures.

The inclusion of a back-up bar continuously fillet-welded to the north tie girder flange and web significantly reduced the calculated bending stresses induced in the web. This occurred because of the increased section properties available at the rigidly fixed web-flange connection. The structural contribution was negligible for the back-up bar connected to the web only by the web-flange groove weld (south tie). This second condition was modeled by complete removal of the back-up bar from the models.

Even though the back-up bar was found to be successful in reducing the web stresses, it was not the solution to the web bending problem; it simply transferred the bending stresses to the back-up bar and fillet welds.

CONCLUSIONS

The following conclusions are made:

1. Web gap movements on the order of thousandths-of-an-inch caused the high stresses capable of producing fatigue cracking.
2. The measured web gap stresses could only be reproduced within the bottom web gaps by placing a floorbeam gap between the floorbeam and the tie girder flange.
3. The closest reproduction of measured stresses occurred with the floorbeam gap extended to the bottom of the tie girder diaphragm.
4. The inclusion of the diaphragm retrofit in the finite element analysis models reduced the web-flange weld root stresses at locations other than the bottom interior corner by one-half to one-fifth of their original values.
5. A tie plate (i.e., floorbeam retrofit) was required to transmit the floorbeam flange force directly into the tie girder flange. With the combined floorbeam and diaphragm retrofits, the bottom interior web gap stresses were reduced to ± 1 ksi when two adjacent directional lanes of HS20 trucks were positioned over the floorbeam. The bottom exterior web gap stresses were essentially eliminated.
6. The retrofit details shown in Figure 4 (taken from contract drawings) implemented all stress-range reducing techniques developed in the study. The particular details are for a tie girder section without a field splice. Similar, but somewhat more complex, detailing was required at tie-girder field splices.
7. The diaphragm stress field was redirected from the diaphragm-web fillet weld to the diaphragm retrofit (not a fatigue-critical connection) and the bottom flange retrofit.
8. The computed web bending stresses at the web-flange weld root doubled when the back-up bars were removed from the models. The back-up bars in the south tie were not continuously fillet-welded to the flange or web and, as such, provided little additional support (essentially removed) to the web. This is of no consequence once the retrofits are provided.

Publication of this paper sponsored by Committee on Steel Bridges.